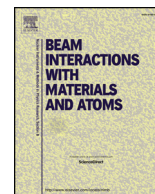




Contents lists available at ScienceDirect

## Nuclear Inst. and Methods in Physics Research B

journal homepage: [www.elsevier.com/locate/nimb](http://www.elsevier.com/locate/nimb)

## Carbon-14 content in tree and soil samples at the Idaho National Laboratory nuclear site

Jessica L. Ward\*, Mathew S. Snow, John E. Olson, Duane Ball, Mary L. Adamic

Idaho National Laboratory, PO Box 1625, Idaho Falls, ID 83415-2805, USA

## ARTICLE INFO

## Keywords:

Accelerator mass spectrometry  
AMS  
Carbon-14  
Idaho National Laboratory

## ABSTRACT

Idaho National Laboratory (INL) is a nuclear research facility located in southeastern Idaho, USA; over the course of its operational history, INL has operated 52 reactors and 1 reactor fuel reprocessing facility. To determine the extent to which previous nuclear operations at INL have impacted local environmental carbon-14 ( $^{14}\text{C}$ ) concentrations, tree and soil samples from the INL desert and surrounding areas were collected, combusted, and analyzed by Accelerator Mass Spectrometry (AMS). Transport models of the plumes from the Advanced Test Reactor Facility (ATR) and the Idaho Chemical Processing Plant (ICPP) suggest the historic annual integrated plume distributions from each of these source terms was most likely in the northeast-southwest direction, with very little ground contact from stack emissions in the immediate vicinity of the facilities and maximum estimated ground contact arising  $\sim 400\text{--}1000\text{ m}$  to the northeast/southwest from each facility.  $^{14}\text{C}$  data from annual growth ring data from trees located immediately adjacent to the ATR, INL's Central Facilities Area (CFA), and Mud Lake, Idaho (ML) are in statistical agreement with regional nuclear weapons testing fallout backgrounds. Surface soil samples taken near a low level radioactive disposal facility and downwind from the ICPP show percent modern carbon (pMC) values ranging from  $28 \pm 2$  to  $92 \pm 4$ , suggesting a mixture of aged and modern background carbon containing materials. Taken together, these data suggest that  $^{14}\text{C}$  in the INL region is predominantly derived from a mixture of aged and modern background sources (e.g. nuclear weapons testing fallout), with insignificant contributions from INL source terms.

## 1. Introduction

Idaho National Laboratory (INL) was established in 1952 for the purpose of developing and testing new nuclear reactor technologies. Since 1952, INL has operated 52 different reactors, a nuclear reprocessing facility (the Idaho Chemical Processing Plant, ICPP) and a nuclear waste management facility (Radioactive Waste Management Complex, RWMC). INL currently has 2 operational reactors (the Advanced Test Reactor, ATR, and Neutron Radiography Reactor, NRAD) and recently restarted a 3rd reactor, the Transient Reactor Test Facility (TREAT) [1].

Evaluation of background environmental radioactivity levels at the INL site is needed prior to future technological demonstrations at INL including the restarting of the TREAT reactor. Documented radionuclide emissions at INL include airborne emissions from reprocessing operations at the ICPP [2], emissions from reactor accidents [3,4], and releases from flooding at the RWMC [3,5,6]. Furthermore, while current emissions are maintained under strict regulatory controls, many historic emissions prior to 1972 are believed to have occurred but were

not monitored [7]. Significant efforts have been made to establish baseline actinide (e.g. Pu, U, Np, Am) and fission product (e.g.  $^{90}\text{Sr}$ ,  $^{137}\text{Cs}$ ,  $^{129}\text{I}$ , etc.) concentrations at the INL desert and surrounding areas [5,6,8,9], however to our knowledge no systematic study of the carbon-14 ( $^{14}\text{C}$ ) content in local vegetation has been performed to date. Therefore, in order to differentiate between legacy operations and potential future emissions, environmental radioactivity analyses are currently needed.

$^{14}\text{C}$  is a radioactive isotope produced in the nuclear fuel, coolant, shielding, and structural materials during nuclear reactor operations [10]. As a beta particle emitter with a half-life of 5730 years [11],  $^{14}\text{C}$  represents a long term dose contributor. Under oxidizing conditions  $^{14}\text{C}$  forms carbon dioxide ( $\text{CO}_2$ ) which can be emitted from a nuclear facility to the atmosphere and subsequently incorporated into local vegetation and fauna, primarily through photosynthetic uptake (for vegetation) and subsequent digestion of vegetation (for fauna) [10,12,13]. When uptaken by trees, a portion of the  $^{14}\text{C}$  is incorporated into the holocellulose for a given annual growth ring, thereby preserving a record of the integrated atmospheric  $^{14}\text{CO}_2$  levels for a given

\* Corresponding author at: 1765 N Yellowstone Hwy, Idaho Falls, ID 83415, USA.  
E-mail address: [jessica.ward@inl.gov](mailto:jessica.ward@inl.gov) (J.L. Ward).

<https://doi.org/10.1016/j.nimb.2018.08.047>

Received 9 January 2018; Received in revised form 19 June 2018; Accepted 30 August 2018  
0168-583X/ Published by Elsevier B.V.

year's growing season (e.g. the longest period of non-freezing temperatures of the year, which for southeastern Idaho is typically from April–May to late September depending on the weather conditions in a given year). Upon death of the vegetation or defoliation, organic carbon molecules are transferred to the soil where they subsequently decompose into other organic and inorganic carbon forms [14].

The total  $^{14}\text{C}$  content in surface soils is derived from various source terms.  $^{14}\text{C}$  produced in the upper atmosphere is continually introduced in soils as  $^{14}\text{CO}_2$  through precipitation and root respiration [15–17]. Once input into the soil,  $^{14}\text{CO}_2$  can be incorporated into inorganic carbonate species through  $\text{CO}_2$  oxidation and subsequent precipitation with soil cations.  $^{14}\text{C}$  that is thus fixated gradually decays to produce  $^{14}\text{C}$  depleted carbonate compounds, with common carbonate mineral formations (including many limestones) containing  $^{14}\text{C}$  content as low as  $\sim 0$  percent modern. Additional  $^{14}\text{C}$  input into soils occurs through the decay of vegetation, where molecular degradation processes result in the breaking down of complex organic molecules into other simpler carbon containing compounds (the uptake of which is subject to isotopic fractionation [28]).

Significant mixing of aged and modern  $^{14}\text{C}$  can occur in surface soils through a combination of Aeolian, pluvial, and biochemical processes. Mixing between inorganic carbonates is facilitated through the formation of secondary carbonate precipitates, where modern  $^{14}\text{CO}_2$  in soil and aged carbonate minerals are dissolved and transported vertically (and laterally) through sediment layers via the influx of rainwater, and are subsequently deposited upon evaporation [16,18,19]. At the soil-atmospheric interface, mixing of various carbon species occurs through weathering/erosion processes and wind-driven particulate transport. Further microbial and biological interactions above and below the soil-atmospheric interface can contribute to carbon cycling [15]. The net result is a complex, dynamic system of mixing between modern (e.g.  $\sim 100\%$  pMC for cosmogenic  $^{14}\text{C}$ ,  $> 100\%$  pMC for anthropogenic) and aged ( $\sim 0$  pMC) carbon containing constituents.

This work reports the  $^{14}\text{C}$  concentrations in soils and individual annual growth rings from trees located on or near the INL site. Sampling locations were selected based upon their proximity to major potential emission source terms including ATR, ICPP, and RWMC.  $^{14}\text{C}$  analyses from tree rings are further compared with reported historic emissions and meteorological data to assess whether trees at the INL site and nearby environment can be utilized to infer whether significant emissions occurred prior to the 1970s.

## 2. Methods

### 2.1. Environmental sampling

The INL site is an 1158 km<sup>2</sup> reserve located on the upper Snake River Plain in south-eastern Idaho (Fig. 1). On average, the site has only 22 cm of precipitation per year classifying the site as a semiarid climate [6,8]. Average wind speeds at the INL site were 11.5 km/hour during a 14 year period with monthly highs ranged from 96.5 to 125.5 km/hour primarily NE-SW directions, with the strongest winds originating from the south-west direction [6,8,20].

The locations of the sampling sites from this study are given in Fig. 1. Tree sampling locations were selected based on the location of major suspected legacy emission sources (e.g. the ICPP and ATR), predominant wind directions and the availability of aged trees at the site. The samples collected from the ATR site were cross sections obtained from a pine tree that fell down  $\sim 4$  m from the ATR reactor building in 2016. For tree samples near the Central Facilities Area (CFA) and Mud Lake (ML), tree core samples were taken at waist height using a 0.25" Haglof tree coring tool. The trees sampled from both ATR and CFA are believed to be non-native to the INL desert and may have been transplanted from nurseries during the early 1970's as indicated through analyses of historic documents [21]. On the other hand, the core taken from a cotton wood tree near ML is believed to be native to the lake.

Soil samples were collected in July 2012 from surface locations (0–8 cm in depth) using a hand trowel, with the exception of sample BG 1–4 which was taken from a 0–4 cm depth in 1974 [6]. The soils and sediments were passed through a mesh screen in the field to remove rocks and debris larger than 1 cm in size. The samples were then dried and large particulates were physically removed using tweezers prior to subsequent combustion.

### 2.2. Tree sample sectioning and dendrochronology

After collection, tree core and cross section samples were dried in a laboratory oven at 100 °C and lightly sanded using 220 grit sandpaper. The cores were then lightly sprayed with canned air (Air Power Dusters, Compucessory) to remove sawdust and other potential particulate impurities. Samples were evaluated visually and (when necessary) via a light microscope to identify annual growth ring boundaries and assign dates to each ring. Visual analyses were determined to be most appropriate for the CFA and ATR samples as these trees were suspected to have been hand watered at INL and thus their annual growth ring widths would not correspond with master chronologies for pine trees in the southeastern Idaho region. Ring widths for CFA and ATR samples were fairly wide (20–150 mm) and no evidence of false or missing rings were observed. An absence of false or missing rings were also observed for the ML tree cores, however comparisons of  $^{14}\text{C}$  data from this tree to data reported for nuclear weapons testing backgrounds in the northern hemisphere strongly suggested that there may have been a missing ring between rings 47 and 48, as adjustment of the dates for rings after 47 by 1 year results in perfect agreement with fallout background data. Thus, data from tree rings older than 47 years in the ML tree were adjusted accordingly (see Table SI-3, SI-4 and SI-5, Supporting information for raw  $^{14}\text{C}$  data from each tree as a function of the ring number and assigned ring year).

After assigning dates, individual annual growth rings were separated from each other using a chisel and a hammer and sliced into fine pieces using a razor blade, with cuts performed normal to the direction of annual growth in order to capture a sample of the entire annual growth season in each slice. Between sectioning each set of annual growth rings, sectioning tools were washed with ethanol (200 proof, HPLC grade, Sigma Aldrich, MO), wiped with Kimwipes and dried with canned air. Additionally, brand new layers of aluminum foil (Great Value, AK) were utilized as a clean surface between each sample. After sectioning, slices were transferred into filter bags (F57 filter, Ankom Technology) that were heat sealed in preparation of sample treatment process.

### 2.3. Tree sample treatment process

The holocellulose fraction of each tree ring was isolated using the Soxhlet extraction-bleach procedure of Southon et al. [22]. The bagged samples were placed in a soxhlet apparatus and were treated for 18 h with a 2:1 solution of toluene: ethanol followed by an additional 18 h of pure ethanol. The bagged samples were then washed in a 17.8 M $\Omega$  water bath, lightly refluxed and covered by a watch glass for three hours. Following water treatment, samples were bleached with 1.3 g sodium chlorite (80% purity, Sigma Aldrich) and 0.670 ml glacial acetic acid (99.99% purity, Sigma Aldrich) in 200 ml of 17.8 M $\Omega$  water for 3 h at 70 °C followed by an additional bleaching treatment using 1.3 g sodium chlorite and 0.670 ml of glacial acetic acid for 12–18 h. After bleaching, samples were rinsed three times with 17.8 M $\Omega$  water and dried in a vacuum oven at 50 °C for 3 h. Bags were then stored in aluminum foil lined air tight plastic containers prior to AMS sample preparation.

### 2.4. Sample combustion, graphitization and AMS cathode preparation

Samples were converted to  $\text{CO}_2$  following the combustion procedure of Southon et al. [23]. To minimize blank  $^{14}\text{C}$  levels, quartz combustion

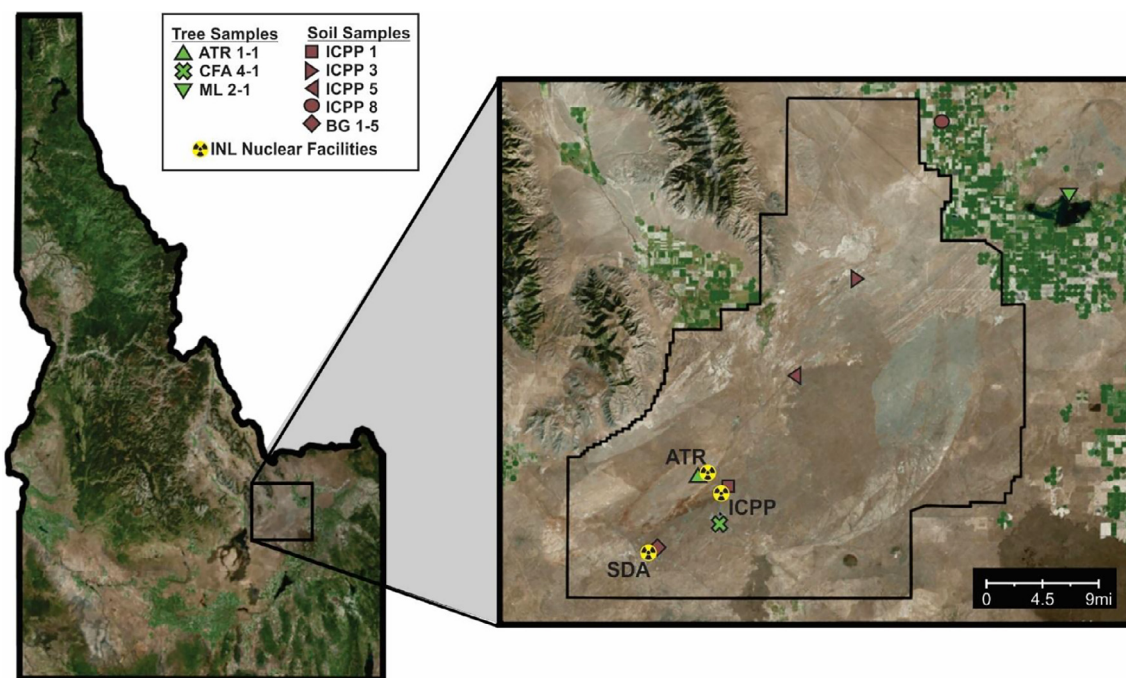


Fig. 1. Map showing the location of the INL site within the state of Idaho, USA. Major nuclear facilities and locations of tree and soil samples are further indicated.

tubes (18 cm long  $\times$  6 mm O.D.) and copper oxide (ACS grade, Fisher Chemical) were baked at 900 °C and silver wire ( $\leq 0.024$  g, 99.9%, Alpha Aesar) was baked at 500 °C in preparation for combustion tube assembly [24]. Tree samples (0.0050–0.0085 g) and soil samples (0.02–0.06 g) were then placed into the combustion tubes along with 0.180 g of copper oxide and a small piece of silver wire. Quartz tubes were evacuated to a pressure of 1–2 millitorr, flame sealed using an oxygen propane torch, placed in a muffle furnace and heated at 900 °C for four hours.

Upon combustion, samples were graphitized using the Zn/TiH<sub>2</sub> reduction method of Xu et al. [25]. The graphitization process utilized an outer 13.5 cm  $\times$  84 mm Pyrex tube with a slight dimple at  $\sim 110$  mm from the bottom and a 50 mm  $\times$  6 mm inner Pyrex tube, both of which were prebaked at 500 °C. Zn (0.012–0.015 g) (Aldrich, 99.995%) and TiH<sub>2</sub> (0.04–0.06 g) (Alfa Aesar, 99%) were then added to the bottom of the larger Pyrex tube and Fe powder (0.012–0.016 g) (Alfa Aesar, 98%, LOT# K20Z075) was added to the smaller Pyrex tube, following which the complete graphitization tube assemblies were prebaked at 275 °C for 3 h [24].

A general schematic of the vacuum manifold utilized for sample combustions/graphitization is given in Figure SI-1, Supplementary Information. Combusted sample tubes were placed inside a flexible vacuum bellows tube, following which the manifold was evacuated and gases produced during combustion were introduced into the manifold by bending the bellows until the glass tube shattered. Combustion gases were then passed through a dry ice/methanol bath to trap the excess water and a liquid nitrogen trap for collecting CO<sub>2</sub>. Upon complete transfer of CO<sub>2</sub>, non-condensable gases were evacuated from the system, CO<sub>2</sub> was transferred cryogenically to a graphitization tube and flame sealed. Graphitization tubes were then baked at 500 °C for 4 h and then 550 °C for an additional 4 h, following which the outer graphitization tubes were scored and cracked open and the iron/graphite mixtures were pressed into titanium cathodes in preparation for AMS analysis.

### 2.5. AMS data reduction/standards analysis

<sup>14</sup>C analyses were performed using a 0.5 MV compact AMS system manufactured to INL's specifications by the National Electrostatics

Corporation. <sup>12</sup>C/<sup>14</sup>C and <sup>12</sup>C/<sup>13</sup>C isotope ratio measurements were corrected for isotopic fractionation using NIST-4990C (Oxalic Acid-II). Other secondary standards including IAEA-C7 (oxalic acid), IAEA-C3 (cellulose), and Alpha Aesar graphite ( $\alpha$ , 99.9999%) were analyzed on each wheel for quality assurance, dead carbon, and modern carbon background corrections (respectively). To maximize measurement precision, replicate cathodes (2–3) of each sample/standard were analyzed on each wheel, with the final <sup>12</sup>C/<sup>14</sup>C ratio reported representing the combined data from replicate cathode measurements. Final data reduction (including  $\delta^{13}\text{C}$  and process background corrections) were performed using the NEC abc AMS software (with the definition of pMC reported as the measured activity ratio of the sample to that of OXI as described in detail in Stenstrom et al. (equation 31) [28]).

### 2.6. ICPP and ATR emission plume modeling

Estimation of the average integrated airborne plumes from the ATR reactor and ICPP reprocessing facility were performed using BEEST version 11.07 program with the EPA AERMOD 16216r and associated modules (ORIS-solutions, Providence Engineering and Environmental Group LLC). Data for stack heights and air flow from each stack were obtained from Rood and Sondrup [26]. Large area plume geographical distributions were modeled using 1 in: 110 m scale. An arbitrary assumption of 4.5 kg/hr CO<sub>2</sub> emissions was assumed in order to generate general plume distributions from each stack. Wind patterns were modeled using annual integrated airflow data from the Boise weather station (for airflow heights > 16.2 m from ground level) and from the Rexburg weather stations (for airflow heights < 16.2 m from ground level).

## 3. Results

### 3.1. Method validations

Analyses of IAEA-C3 and IAEA-C7 reference materials for combustion, graphitization, and instrumentation method validations are shown in Fig. 2 and Table SI-2 (Supplementary Information).

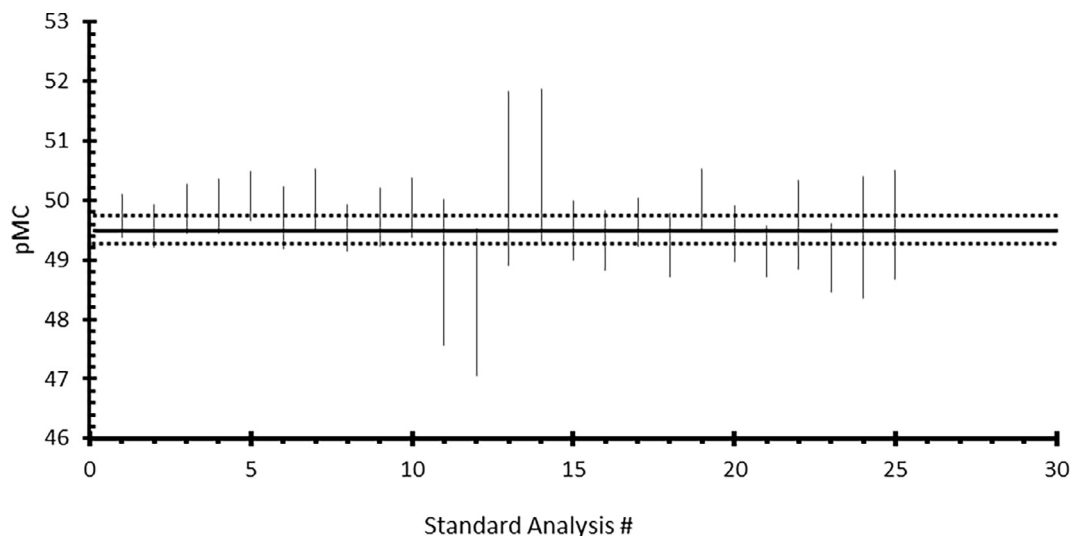


Fig. 2. Measured values for the secondary standard IAEA-C7 (oxalic acid). Uncertainties represent  $2\sigma$  uncertainties for individual sample measurements.

Individual analyses of each standard are found to agree with certificate values, thereby strengthening confidence in the values obtained for subsequent unknown samples in this work. Assessment of modern carbon blank levels using Alpha Aesar graphite revealed process backgrounds on the order of 1 pMC. While these blank levels are suspected to result primarily from low level carbon blank within the specific batch of Fe utilized in this work, process backgrounds were sufficiently low and consistent to enable effective correction using the NEC data evaluation software (as evidenced by the agreement within uncertainty between measured and certificate values for IAEA-C7 and IAEA-C3).

### 3.2. ICPP and ATR gaseous transport model predictions

BEEST plots showing the estimated annual integrated plume distributions from ATR and ICPP are given in Fig. 3. The predominant plume direction from both facilities is predicted to be primarily in the northeast-southwest direction, consistent with experimentally observed particulate transport at the INL site [6]. Due to the large stack heights of ICPP and ATR (67.5 m tall), little plume contact at ground level is predicted in the immediate vicinity of each facility, particularly to the southeast. Maximum contact of the plumes from ATR and ICPP with the ground is predicted roughly 400–1000 m to the northeast of each facility. As the exact airborne plume patterns are a function of the actual quantities of  $^{14}\text{CO}_2$  emitted and the specific meteorological conditions at a given time, the trends described above represent first approximations to the expected  $^{14}\text{C}$  distributions from each facility, to be verified with experimental measurements from field samples.

While locations ~400–1000 m to the northeast and southwest of ATR and ICPP are predicted to be ideal for capturing the plumes from these source terms at ground level, the INL site is a desert and no trees were available at these locations. Thus, though not predicted to be ideal with respect to location relative to the primary plumes, tree samples were collected at CFA and next to the ATR building as they represented the nearest available trees. Additionally, while Mud Lake is 64 km to the northeast of ATR/ICPP and thus is relatively distant from these facilities, it represents the nearest location in the predominant plume direction that contained trees. On the other hand, soil sample collection within the primary plume pathway was

possible and thus samples were collected with systematically increasing distances to the northeast of the ICPP/ATR (samples ICPP 1 through ICPP 8).

### 3.3. INL soil data

Measurements of the total  $^{14}\text{C}$  content in surface soils at the INL site are given in Table 1. Values for soils are found to range from  $28 \pm 2$  to  $92 \pm 4$ , which is within the broad range predicted for mixing between aged and modern background source terms. Specifically, a lack of measurable increase above 100 pMC in  $^{14}\text{C}$  in soil samples indicates that  $^{14}\text{C}$  emissions from the ICPP, ATR, and possible fugitive releases from the Subsurface Disposal Area (a low level radioactive waste disposal area that experienced numerous flooding and fire events since 1952) are not able to be distinguished from fluctuations in the local background  $^{14}\text{C}$  content in surface soils at the locations investigated. As surface soils in this work are within the ideal plume deposition area from all 3 of these major source terms, the lack of observed INL derived  $^{14}\text{C}$  could be caused by several factors including 1) emissions of  $^{14}\text{C}$  from all 3 source terms were negligible relative to other background sources and 2) the residence times of plumes from each source term were not sufficient to result in significant exchange (via direct  $\text{CO}_2$  and biochemical processes) with carbon species in the local soils. It is also important to note that if significant  $^{14}\text{C}$  emissions occurred during winter months such emissions would not likely have been captured in local flora or soils due to the minimal  $^{14}\text{CO}_2$  capture by local vegetation during the winter months.

### 4. Southeastern Idaho tree ring data

Tree ring data collected from trees at CFA, ML, and ATR are shown in Fig. 4 and Table 1 (see also Fig. 5). Data are observed to fall directly on the global fallout curve for the Northern Hemisphere Zone 2 reported by Hua et al. [27]. These data indicate that the annual integrated atmospheric  $^{14}\text{C}$  content at each of these locations is indistinguishable from background, non-INL sources (e.g. natural production + global nuclear weapons testing).

The lack of INL derived  $^{14}\text{C}$  in the ML 2-1, ATR 1-1, and CFA 4-1 tree samples could be the result of several factors. First, plume modeling efforts described in Section 3.2 suggest that very little ground contact of

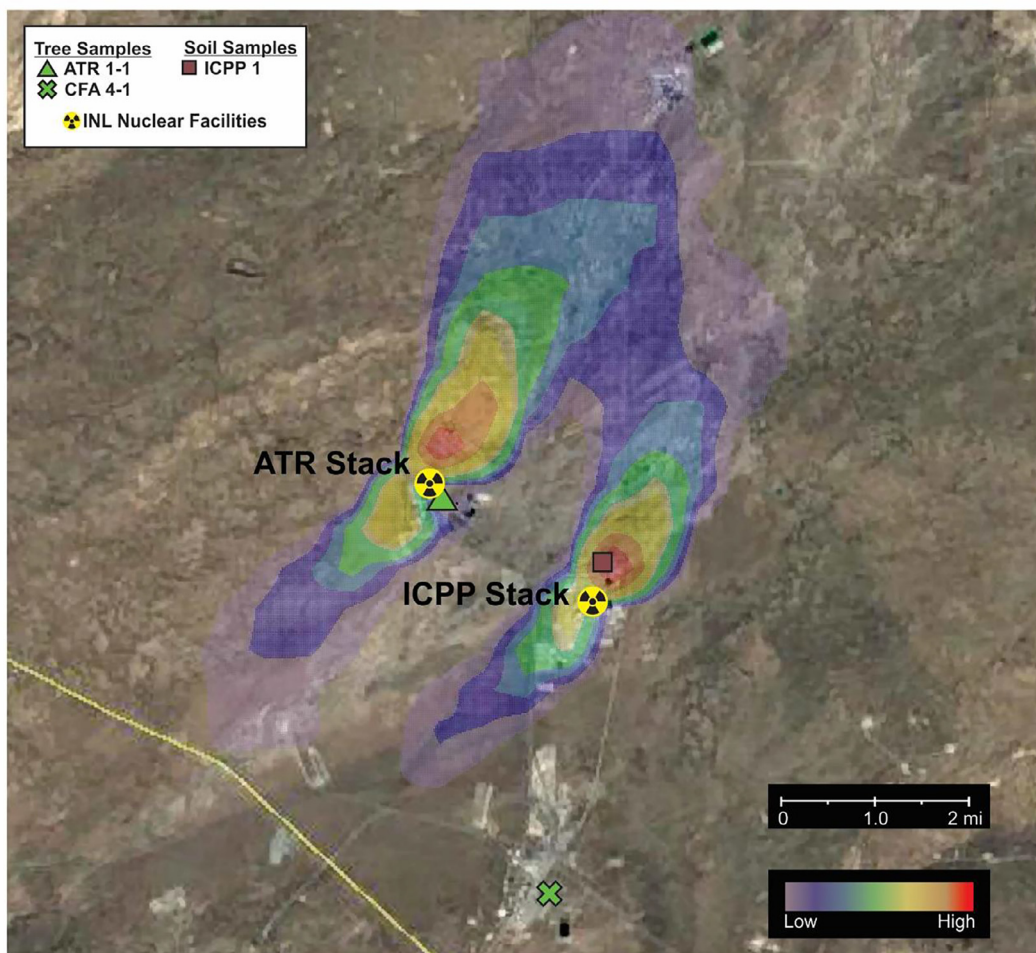


Fig. 3. BEEST plot showing the predicted average plume distributions from ATR and ICPP. Plume distribution predictions are based upon integrated annual wind data from Rexburg and Boise weather stations (for airflow heights < 16.2 m and > 16.2 m from ground surface respectively) and are intended to represent general emission patterns anticipated from these facilities only.

**Table 1**

Measured pMC data from INL surface soil samples. Uncertainties represent  $2\sigma$  replicate uncertainties.

| Soil ID | pMC         |
|---------|-------------|
| BG1-5   | $87 \pm 4$  |
| ICPP-1  | $60 \pm 25$ |
| ICPP-3  | $92 \pm 4$  |
| ICPP-5  | $28 \pm 2$  |
| ICPP-8  | $65 \pm 9$  |

the plume occurred directly to the southwest of ATR where the ATR tree was located ( $\sim 4$  m from the facility). In the case of the CFA tree, the primary plume from ICPP is predicted to have passed immediately to the north of CFA and thus CFA 4-1 most likely only had intermittent contact with the fringes of this plume (if significant contact occurred at all). Finally, while ML 2-1 was located within the main plume path for ATR and ICPP, its location (64 km northeast) is at sufficient distance that  $^{14}\text{CO}_2$  from ATR and ICPP may have been diluted to levels indistinguishable from background nuclear weapons testing/cosmogenically derived  $^{14}\text{CO}_2$ . The apparent ideal location of a sample would have been located at  $\sim 400$ – $1000$  m distance to NE from ATR/ICPP, however

as the INL site is a desert, no trees are available in the ideal region (only sagebrush, which frequently turns over due to frequent fires on desert). Therefore, data from this study indicates that INL operations have caused insignificant impact to local annual integrated  $^{14}\text{C}$  levels in the trees at the locations investigated.

## 5. Conclusion

To determine the impact of INL nuclear operations upon the local environmental  $^{14}\text{C}$  content, tree and soil samples from the INL desert and surrounding areas were collected, chemically processed and analyzed using accelerator mass spectrometry. Total  $^{14}\text{C}$  in soil samples varied from  $28 \pm 2$  to  $92 \pm 4$  pMC, suggesting a mixture of aged and modern background carbon sources (e.g. insignificant INL contributions).  $^{14}\text{C}$  data from tree rings, collected from locations near ATR, CFA, and ML, are all found to be in agreement with reported values for northern hemisphere global nuclear weapons testing fallout, suggesting that the  $^{14}\text{C}$  emissions from the INL site resulted in insignificant impact on the long term atmospheric  $^{14}\text{C}$  concentrations at these locations. Taken together, these data provide a general baseline for determining the future impacts of the TREAT reactor and other nuclear facilities in southeastern Idaho.

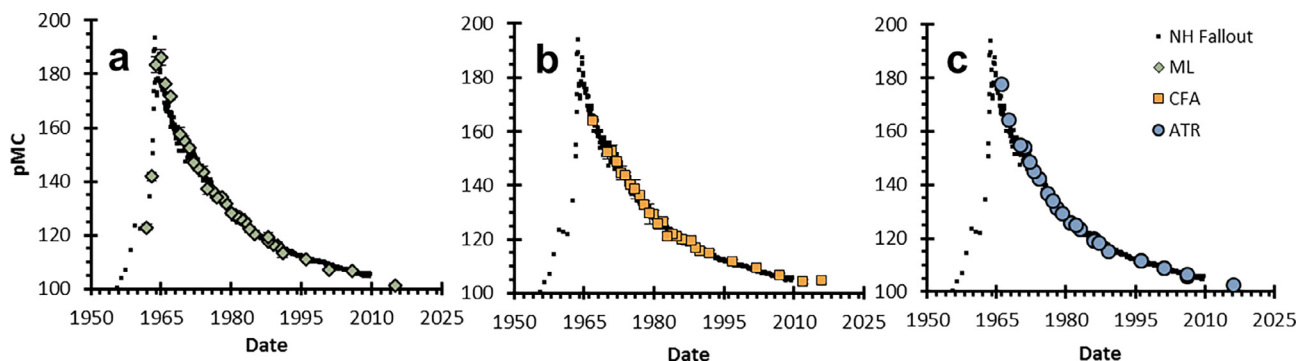


Fig. 4.  $^{14}\text{C}$  data as a function of the annual growth ring for trees a) ML 2-1, b) CFA 4-1, and c) ATR 1-1. Global fallout background data is taken from Hua et al. [23] for the Northern Hemisphere in Zone 2.

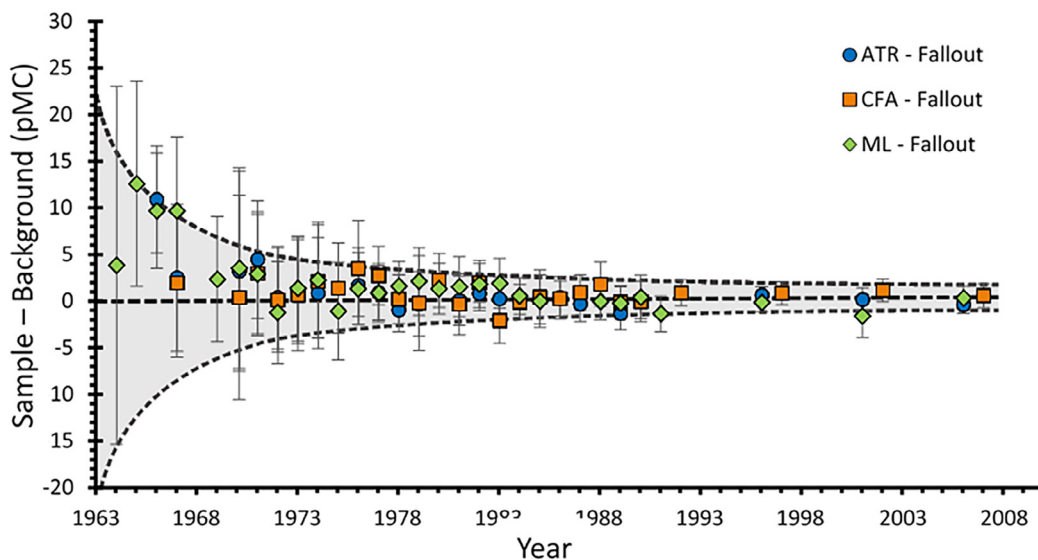


Fig. 5. Comparison of the difference between the pMC detected in annual growth rings from trees near the INL site to that of Northern Hemisphere fallout. Gray shaded area represents the approximate average  $\pm 2\sigma$  variation in annual regional background pMC given by Hua et al. [27] Data are observed to fall within the mean  $\pm 2\sigma$  of the variation in the Northern Hemisphere fallout for a given annual growth ring.

## Acknowledgements

The authors would like to thank Dr. John Southon, Dr. Xiaomei Xu, and Dr. Guaciara M. Santos from the University of California-Irvine for their assistance with establishing and improving the  $^{14}\text{C}$  analysis capabilities at Idaho National Laboratory; Jacob Gray from Idaho Fish and Game for assistance with collecting the Cottonwood tree cores at Mud Lake; Dr. Darin Snyder for collection of the ICPP soil samples; and Mike Sandvig, Rod Mason, and Brett Lewis for collection of the ATR cross section and CFA tree core samples. Work was supported through the INL Laboratory Research & Development (LDRD) Program under DOE Idaho Operations Office Contract DE-AC07-05ID14517.

## Appendix A. Supplementary data

Supplementary data associated with this article can be found, in the online version, at <https://doi.org/10.1016/j.nimb.2018.08.047>.

## References

- [1] K. Trevelyan, INL to Restart Test Reactor, Post Register, 2017.
- [2] R. Mitchel, R. Brooks, D. Oetersib, L. Paulus, D. Roush, D. Martin, Idaho national engineering and environmental report for calendar year, Environ. Sci. Res. Found. Rep. Series (1996) DOE/ID-12082(96).
- [3] S. Stacy, Proving the Principle a History of the Idaho National Engineering and Environmental Laboratory 1949–1999, DOE/ID-10799, 2000.
- [4] M. Swanson, M. Reed, T. Fedor, Transformed: A Recent History of the Idaho National Laboratory 2001–2010, Idaho National Laboratory, 2012.
- [5] M. Snow, D. Snyder, S. Clark, M. Kelley, J. Delmore,  $^{137}\text{Cs}$  activities and  $^{135}\text{Cs}/^{137}\text{Cs}$  isotopic ratios from soils at Idaho National Laboratory: a case study for contaminant source attribution in the vicinity of nuclear facilities, Environ. Sci. Technol. (2015).
- [6] D. Markham, K. Puphal, T. Filer, Plutonium and americium contamination near a transuranic storage area in southeastern Idaho, J. Environ. Qual. (1978).
- [7] INEL, A Comprehensive Inventory of Radiological and Nonradiological Contaminants in Waste Buried in the Subsurface Disposal Area of the INEL RWMS during the Years 1952–1983 Vol 4, INEL-95/0310, 1995.
- [8] T. Beasley, J. Kelley, L. Bond, W. Rivera, M. Liewiski, K. Orlandini, Heavy element radio nuclides (Pu, Np, U) and  $^{137}\text{Cs}$  in soils collected from the Idaho national engineering and environmental laboratory and other sites in Idaho, Montana and Wyoming, Environ. Meas. Lab., EML-599 (1998).
- [9] T. Beasley, P. Dixon, L. Mann,  $^{99}\text{Tc}$ ,  $^{236}\text{U}$ , and  $^{237}\text{Np}$  in the snake river plain aquifer at the Idaho national engineering and environmental laboratory, Idaho Falls, Idaho, Environ. Sci. Technol. (1998).
- [10] W. Davis, Carbon-14 Production in Nuclear Reactors, U.S. Nuclear Regulatory Commission, 1977.
- [11] H. Godwin, Half-life of Radiocarbon, Nature (1962).
- [12] M. Carbon O'Leary, Isotopes in Photosynthesis, BioScience (1988).
- [13] L. Weisser, J. Salmond, L. Schwendenmann, Photosynthetic  $\text{CO}_2$  uptake and carbon sequestration potential of deciduous and evergreen tree species in an urban environment, Urban Ecosyst (2016).
- [14] J. Balesdent, G. Wagner, A. Mariotti, Soil organic matter turn over in long-term field experiments as revealed by carbon-13 natural abundance, Soil Sci. Soc. Am. J. (1988).
- [15] R. Lal, Sequestration of Soil Carbon as Secondary Carbonates, AGU, 2013.
- [16] R. Lal, Carbon sequestration in soil, Perspect. Agric., Vet. Sci., Nutr. Nat. Resour. (2008).
- [17] H. Craig, The geochemistry of the stable carbon isotopes, Geochimica et Cosmochimica Acta (1952).
- [18] H. Scharpenseel, H. Schiffmann, Soil radiocarbon analysis and soil dating, Geophys. Surv. (1977).
- [19] J. Balesdent, G. Wagner, A. Mariotti, Soil organic matter turnover in long-term field experiments as revealed by carbon-13 natural abundance, Soil Sci. Soc. Am. J. (1988).
- [20] G. Griffith, S. Hoiland, INL site conditions and properties, INL/EXT-15-36721 (2015).
- [21] D. Miley, American nuclear society names INL's ATR complex a nuclear historic landmark, INL.gov (2017).
- [22] J. Southon, A. Magana, A comparison of cellulose extraction and alpha pretreatment methods for AMS  $^{14}\text{C}$  dating of ancient wood, Radiocarbon (2010).

- [23] J. Southon, et al., UCI KCCAMS Facility, *Combust. Protoc.* (2004).
- [24] G. Santos, X. Xu, Bag of tricks: a set of techniques and other resources to help  $^{14}\text{C}$  laboratory setup, sample processing, and beyond, *Radiocarbon* (2016).
- [25] X. Xu, S. Trumbore, S. Zheng, J. Southon, K. McDuffee, M. Luttgen, J. Liu, Modifying a sealed tube zinc reduction method for preparation of AMS graphite targets: reducing background and attaining high precision, *Nucl. Inst. Methods Phys. Res. B* (2007).
- [26] A. Rood, A. Sondrup, Development and demonstration of a methodology to quantitatively assess the INL site ambient air monitoring network, INL/EXT-14-33194 (2014).
- [27] Q. Hua, M. Barbetti, A. Rakowski, Atmospheric radio carbon for the period 1950–2010, *Radio Carbon* (2013).
- [28] K.E. Stenstrom, G. Skog, E. Georgiadou, J. Genberg, A. Johansson, A guide to Radiocarbon Units and Calculations, Lund University, 2011 LUNFD6(NFFR-3111)/1-17(2011).